ACTA ACUSTICA UNITED WITH ACUSTICA
Vol. 88 (2002) 231 – 238

Reducing Screen-Induced Refraction of Noise Barriers in Wind by Vegetative Screens

T. Van Renterghem, D. Botteldooren
Department of Information Technology, Ghent University, St. Pietersnieuwstraat 41, 9000 Gent, Belgium

W. M. Cornelis, D. Gabriels
Department of Soil Management and Soil Care, Ghent University, Coupure links 653, 9000 Gent, Belgium

Summary
The efficiency of noise barriers in downwind direction is strongly reduced by refraction of sound. This effect has been analysed by many authors both in calculations and in experiments. The question arises whether it is possible to influence the wind-factor and to what extent the performance of the barrier could eventually be increased. This paper reports on a wind tunnel experiment set up to try to answer this question. The experiment focuses on the insertion loss close to the barrier (up to a distance of 10 times the barrier height). A model at scale 1/20 is constructed. Both single and double noise barrier (i.e. a noise barrier on either side of the source) configurations are tested, in combination with windscreens. Scale models of vegetative screens are used to modify wind profiles close to the noise barrier. The positive effect on barrier performance is of the order of a few dB. Although this effect may seem small at first sight, it can be obtained at virtually no additional cost and therefore is of practical interest.

PACS no. 43.28.Fp, 43.50.Vt

1. Introduction

In the atmospheric boundary layer, the air flowing over the earth surface slows down due to friction. In most practical cases the wind velocity increases approximately logarithmically with height in this layer. Above the boundary layer, the wind velocity is independent of the surface and this part of the atmosphere is called the free-stream zone. The height of the top of the boundary layer is quite variable, and ranges from typically 100 m to a few kilometres. This has important consequences for sound propagation. Downwind from a noise source, there will be refraction of sound rays towards the ground. Upwind, a large shadow region is created.

Temperature profiles in the atmosphere also affect the refraction of sound. An increased noise level under temperature inversion conditions is well known. In most practical situations however, the wind effect dominates [1]. Turbulence is also an important environmental influence. Scattering of sound due to a turbulent flow becomes important, especially for sound propagation over long distances and for high frequencies [2].

A reduction of the efficiency of noise barriers in wind has been analysed by many authors [1, 3, 4, 5, 6, 7, 8]. Just behind the barrier, a windless region occurs (underpressure). The (compressed) streamlines just above the barrier are bent down towards the ground. This causes refraction of sound: the acoustic shadow region behind the barrier becomes smaller and the barrier efficiency decreases strongly.

Besides this additional refraction caused by the screen, there is also an increase in turbulence. However, the effect of this turbulence on sound propagation can only be observed in the deep shadow zone, where sound pressure levels are low. There, the contributions of scattered waves are significant [9]. Close to the screen, these turbulence effects are small in comparison with the screen-induced refraction. [8].

Not much effort has been done to cope with the problem of screen induced refraction. Salomons e.g. proposed a different shape of noise barriers, a vented screen. Smooth and more streamlined barriers may also be beneficial in this respect [1]. In this paper, another solution, not focussing on the barrier itself, is proposed. A vegetation screen just behind a barrier is investigated. Since the acceptance of noise barriers is higher for naturally constructed barriers and leads to a decreased annoyance [10], the use of trees behind noise barriers may have positive psychological effects. Besides an improvement of the visual impact of the barrier, the canopy of trees will also influence the wind profile. It will be shown in this paper that an improved wind profile can have a more important beneficial effect than the negative effects caused by scattering on leaves and twigs. However, it will also be shown that designing an op-

Received 12 July 2001,
accepted 26 February 2002.

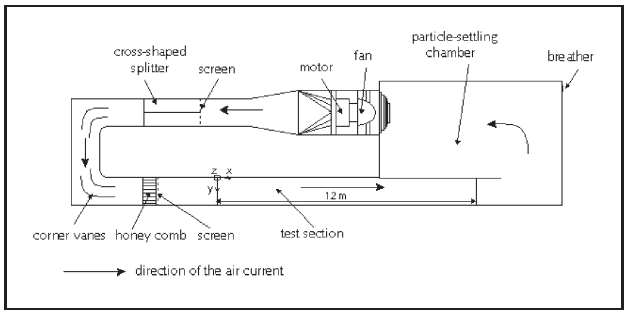

Figure 1. Overview of the I.C.E. wind tunnel.

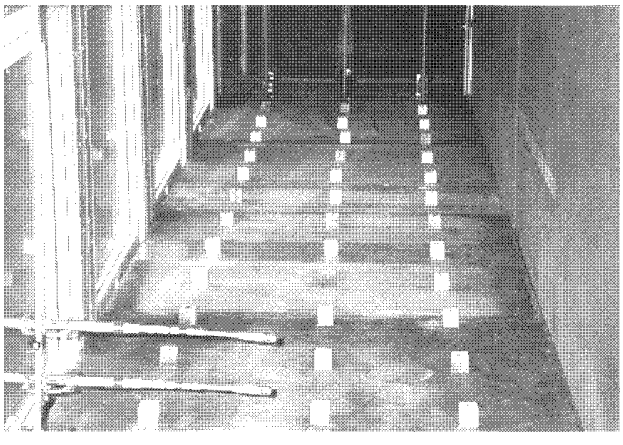

Figure 2. Roughness elements, placed before the test section in the wind tunnel, to raise the top of the boundary layer.

timal wind profile in this way is not a straightforward and easy task.

2. Experimental setup

The experiments were performed in the wind tunnel of the International Centre for Eremology, Ghent University, Belgium [11]. This is a closed-circuit tunnel (see Figure 1): after leaving the test section, the air re-enters the system. Air temperature and humidity will therefore be constant during the experiments. A minimum wind speed of 6.4 m/s can be obtained.

In wind tunnel experiments, it is very important to create a realistic boundary layer. This is however hard to accomplish. Only a large scaling factor (e.g. 100) could solve this problem. But experiments at such a scale would be difficult to perform accurately. Very small microphones are needed, together with a high-precision positioning system, a very smooth wall and floor, etc. To raise the top of the boundary layer in our experiments, roughness elements and spires are placed before the test section in the tunnel, as shown in Figure 2. This results in a boundary layer of approximately 60 cm. Although this is much smaller than the height of the boundary layer in reality, the part that will affect sound propagation (close to the surface where the big gradients occur) is modeled correctly. When noise barriers are present, it is also important that the height of the top of the boundary layer is well above the height of the noise barrier (in our case a few screen heights) for a good modeling of the influence of this obstacle on the wind profile.

Downwind sound propagation over barriers is studied, for normal incidence. A scaling factor of 20 is used. For a good acoustic correspondence between scale model and full scale, frequencies need to be scaled. Since the speed of sound does not scale, the wind speed does neither. This means that refraction in the scale model is realistic. As a consequence, turbulence (Reynolds number) is not scaled properly. As already mentioned, the experiment is performed only close to the barrier (up to a distance of 10 times the barrier height), and therefore it can be assumed that the most important effect will be refraction of sound.

The experimental sound frequencies ranged from 10 kHz till 20 kHz. This means that the frequencies in full scale varied from 500 Hz till 1000 Hz, the frequency range of interest for traffic noise.

In this study, sound propagation in the wind tunnel is two-dimensional. The sidewalls in the tunnel are acoustically hard and act as mirrors. A second condition for two-dimensional propagation is a fully absorbing ceiling. This is easily obtained at the frequencies considered by using a fibrous absorber like rock wool (with a thickness of 5 cm). A narrow opening (8 mm) is cut out in the false floor of the test section in such a way that a coherent line source over the complete width of the tunnel is constructed. Underneath the gap, a loudspeaker box (acoustic hard) is placed, filled with tweeters, emitting a signal between 10 kHz and 20 kHz, consisting of pure tones with frequencies separated by 50 Hz. In this way, the emitted frequencies can be easily distinguished from wind tunnel noise.

The tweeters have a diameter of 25 mm, and emit a constant sound pressure level in the frequency range of interest. The radiation pattern of the tweeters is of minor importance since the dimensions of the box determine the source directivity. Measurements in an anechoic chamber have indicated that this source has a uniform power emission over the full width of the box to within 1 dB.

The false floor of the wind tunnel consists of plywood panels, which have an effective flow resistivity of about 2200 kPa s/m^2. Since flow resistivity may be scaled linearly, the ground has an effective flow resistivity of 110 kPa s/m^2 at full scale. This corresponds to a soil, somewhere between a forest ground and a rough pasture [12]. It has to be mentioned that the used panels were roughened and this results in a much softer surface than expected for plywood. Using the single parameter model, proposed by Delany and Bazley [13], based on measured flow resistivity of fibrous absorbent materials, and widely applied for modeling outdoor soils, the floor in the test section must have an absorption coefficient for normal incidence of 0.31 at 10 kHz and 0.43 at 20 kHz. Comparisons between measurements and simulations of propagation in the absence of both screens and wind have shown that the used floor is well suited to model the desired outdoor surfaces. The noise barriers are made of very hard fibre plates, and have a height of 18 cm and a thickness of 1 cm. The

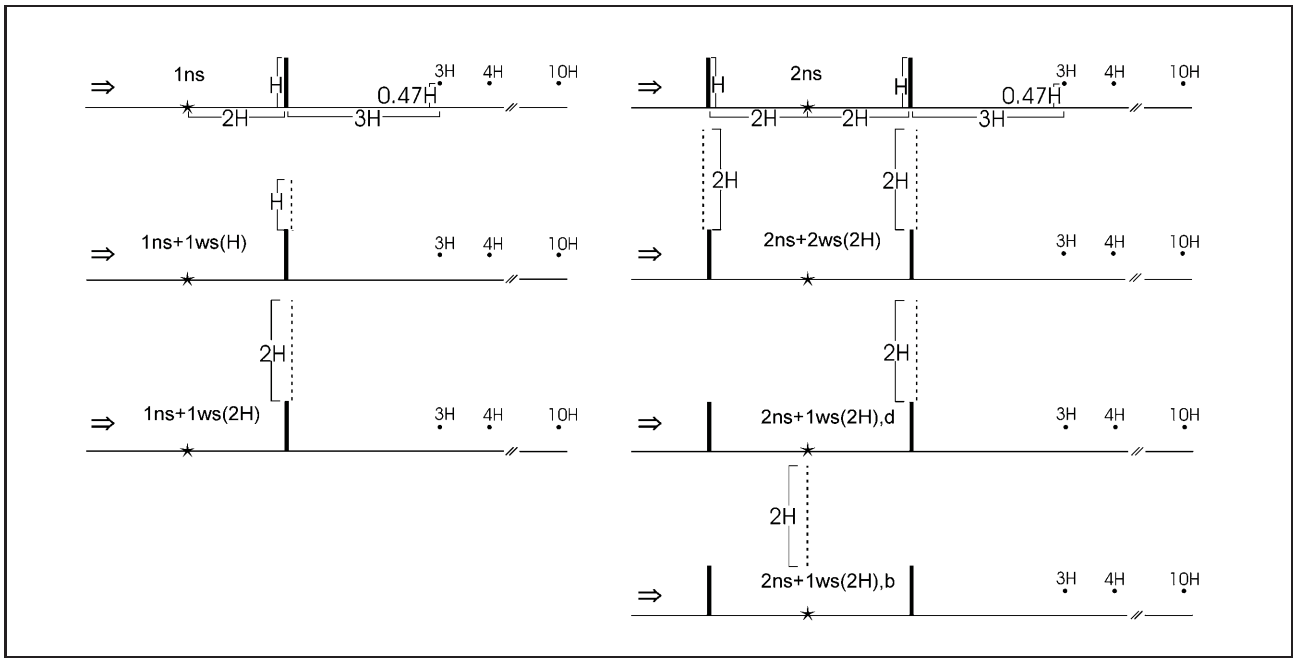

Figure 3. Overview of the tested configurations and dimensions, relative to the noise screen height. The configurations have the following codes: $1ns$ = 1 noise screen; $1ns + 1ws(H)$ = 1 noise screen and 1 windscreen (height of windscreen = barrier height); $1ns + 1ws(2H)$ = 1 noise screen and 1 windscreen (height of windscreen = 2 times the barrier height), $2ns$ = 2 noise screens; $2ns + 2ws(2H)$ = 2 noise screens and 2 windscreens (height of windscreens = 2 times the barrier height); $2ns + 1ws(2H), d$ = 2 noise screens and 1 windscreen (height of windscreen = 2 times the barrier height), placed behind the downwind noise barrier; $2ns + 1ws(2H), b$ = 2 noise screens and 1 windscreen (height of windscreen = 2 times the barrier height), placed between the noise barriers.

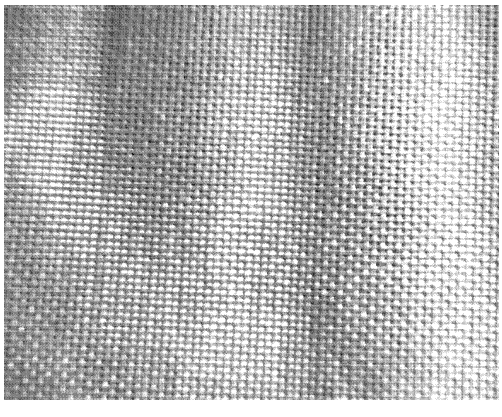

Figure 4. Picture of the windscreens used in the experiment as a scale model for trees.

barriers are placed at a distance of two times the barrier height, downwind and upwind from the line source.

Single noise barriers and double noise barriers (i.e. a noise barrier on either side of the source) are tested, together with different configurations of windscreens. An overview of the tested situations can be found in Figure 3.

A woven windscreen, made of polyester, is used as a scale model for the canopy of trees. A picture of this fabric is given in Figure 4. It has a weight of 230–240 g/m^2 and a tensile strength of 1900 N/cm on wrap and weft. Its elasticity at breakage is about 20%. The screen has uniformly distributed square openings of 1 mm^2. The porosity of this windscreen is 32%. To quantify the overall efficiency of a windscreen in terms of wind speed reduction, the normalized total reduction coefficient (TRc_n) is often used, and is defined as

$$TRc_n = \frac{1}{NM} \sum_{i}^{N} \sum_{j}^{M} \left[1 - \frac{u_{ij}}{u_{0ij}} \right], \qquad (1)$$

where i is an index representing a longitudinal distance behind the windscreen, j is an index representing a height above the surface, N is the number of observations along the longitudinal axis, M is the number of observations along the vertical axis, u_{ij} is the measured wind speed in presence of the screen at the place with index ij, u_{0ij} is the measured wind speed in absence of the screen at place ij.

Experiments revealed that a single windscreen with a porosity of about 32%, placed on the ground, results in a maximal total normalized reduction coefficient. This coefficient was calculated over the main area in which windscreens influence the wind profile i.e. heights ranging from 0.125 to 1.25 windscreen heights, and distances ranging from 2 times the screen height upwind from the windscreen to 32 times the screen height downwind from the windscreen [14]. In literature on windbreaks, values of optimal porosity for overall wind speed reduction range from 25% to 45%.

To model the windscreen, the pressure drop as a function of wind velocity is important. Measurements in the velocity range of interest have indicated that the pressure drop over the windscreens in our test setup can be described with high correlation ($R^2 = 99.6\%$) by the following quadratic equation:

$$\Delta p = av^2 + bv, \tag{2}$$

with $a = 5.040\,\mathrm{Pa\,s^2/m^2}$ and $b = 0.092\,\mathrm{Pa\,s/m}$ [15].

The material is firmly attached over the width of the wind tunnel, so the inevitable bending of the screen (in the middle) due to the wind is restricted to the natural movement of trees in wind (taking the scale factor into account).

The pressure field is measured with a 1/2-inch Bruel and Kjaer microphone (type 4190), with a flat response (± 1 dB) up to 20 kHz for normal incidence. The microphone can be placed with high precision at selected locations behind the downwind barrier. Distances ranged from 3 times the barrier height up to 10 times the barrier height. The microphone is placed $0.47H$ (H = barrier height) above the surface (8.5 cm at scale). This corresponds to the average height of the human ear in full scale (with a scaling factor of 20).

For a free-stream wind speed of 11 m/s, measured above the boundary layer, the background noise level in the tunnel amounts to 85 dB at a frequency of 1 kHz, 50 dB at 10 kHz and 20 dB at 20 kHz. Therefore it is quite easy to generate experimental sound levels well above this background level. To average out short-term fluctuations in the propagation parameters, 20 independent samples were averaged during a period of about half a minute.

Wind velocities are measured with 16 mm vane probes, with a precision of ± 0.1 m/s. Only positive horizontal wind speeds can be measured with the available vanes. Wind velocities are measured with a frequency of 1 Hz and are averaged over a sample period of one minute. These values are then used to calibrate the Computational Fluid Dynamics (CFD) package STAR-CD [16] to obtain more detailed information on the air movement in the tunnel. A logarithmic wind speed profile is imposed as a boundary condition, using equation (3).

$$\ln z = \frac{\kappa}{u_*} v_z + \ln z_0, \tag{3}$$

where z is the height above the surface, v_z is the velocity at height z, κ is the Von Karman constant ($= 0.4$), u_* is the friction velocity and z_0 is the roughness length. At 3 cm, 8.5 cm, 18 cm, 28.5 cm and 42.5 cm above the surface, wind velocities are measured in the wind tunnel (without noise barriers) for a wind speed of 11 m/s (measured above the boundary layer). The parameters in equation 3 are deduced from a curve-fit on these experimental results and yielded $u_* = 0.77$ m/s and $z_0 = 1$ mm. The windscreens are modeled with the porous media flow option of STAR-CD, using parameters a and b to describe the pressure drop over the screen (see equation 2).

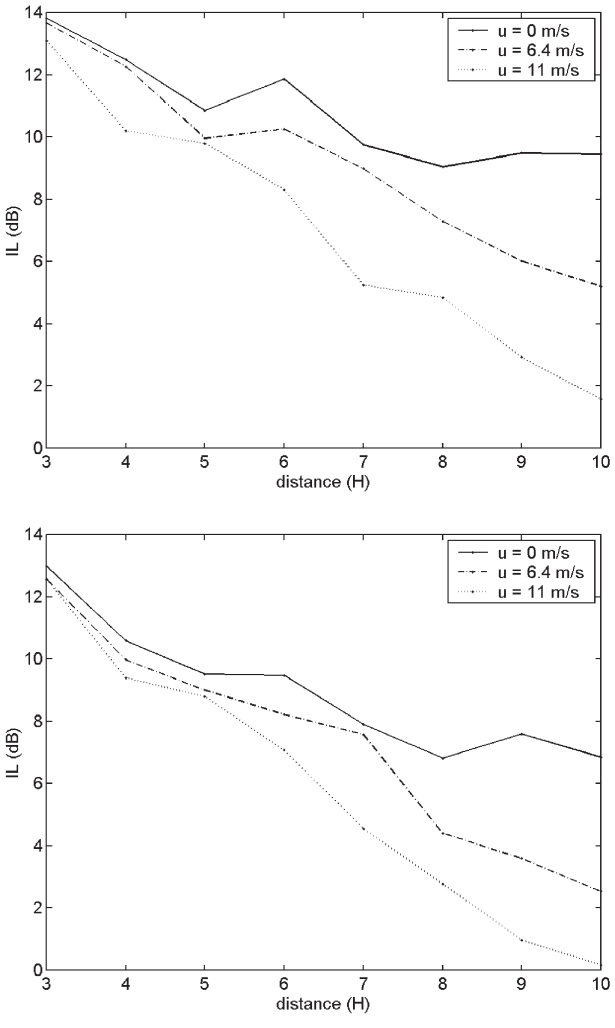

Figure 5. Insertion loss as a function of distance behind the (downwind) noise barrier (expressed in screen heights), for configuration $1ns$ (above) and $2ns$ (below). In both cases, no windscreens are used. The wind velocities above the boundary layer are 6.4 m/s and 11 m/s. To compare, the insertion loss for a windless situation is given.

3. Results and discussion

3.1. General

The performance of a barrier configuration is quantified by its insertion loss (IL), defined as the sound pressure level (SPL) in absence of a barrier minus the SPL with a certain barrier configuration, at the same place, for the same wind speed above the boundary layer. In Table I, an overview is given of the IL (averaged over the used frequency band 500 Hz to 1000 Hz in full scale) for the different configurations of noise barriers and windscreens, together with the wind speeds above the boundary layer.

In the experiment, wind speeds of 6.4 m/s and 11 m/s are used. Although these wind speeds might seem high, it has to be noticed that they are measured above the boundary layer in the wind tunnel. Meteo data recorded at a height of 10 m above a flat terrain (near Aalst in Belgium), thus well within the boundary layer, revealed that one third of the

Table I. Measured IL (in dB) at the test distances (expressed in screen heights), together with the averages over the first part ($av_1 = 3H$–$6H$) and second part ($av_2 = 7H$–$10H$) of the test section, and a global average ($av = 3H$–$10H$). A windless situation ($= u_0$) and two speeds, measured above the boundary layer, are used: $u_1 = 6.4$ m/s, and $u_2 = 11$ m/s.

u_0	$1ns$	$1ns + 1ws(H)$	$1ns + 1ws(2H)$	$2ns$	$2ns + 2ws(2H)$	$2ns + 1ws(2H), d$	$2ns + 1ws(2H), b$
$3H$	13.8	14.0	13.7	13.0	12.8	12.6	12.6
$4H$	12.5	12.4	13.3	10.6	11.5	11.4	10.9
$5H$	10.8	10.4	10.4	9.5	8.2	9.3	8.9
$6H$	11.9	12.1	11.9	9.5	9.3	9.6	9.5
$7H$	9.8	10.2	9.4	7.9	7.1	7.8	7.5
$8H$	9.0	9.1	9.4	6.8	7.4	7.8	7.2
$9H$	9.5	10.1	9.7	7.6	8.3	7.2	7.6
$10H$	9.4	9.7	8.6	6.8	6.7	7.4	6.9
av_1	12.3	12.2	12.3	10.6	10.5	10.7	10.5
av_2	9.4	9.8	9.3	7.3	7.4	7.6	7.3
av	10.8	11.0	10.8	9.0	8.9	9.2	8.9
u_1	$1ns$	$1ns + 1ws(H)$	$1ns + 1ws(2H)$	$2ns$	$2ns + 2ws(2H)$	$2ns + 1ws(2H), d$	$2ns + 1ws(2H), b$
$3H$	13.7	13.4	14.2	12.6	13.1	11.8	12.6
$4H$	12.3	11.9	12.0	10.0	10.4	11.2	10.4
$5H$	10.0	10.9	10.5	9.0	9.4	8.6	9.6
$6H$	10.3	10.6	10.6	8.2	8.2	8.2	8.4
$7H$	9.0	9.7	9.9	7.6	7.3	8.6	6.9
$8H$	7.3	7.5	7.3	4.4	5.4	6.9	5.4
$9H$	6.0	7.0	7.1	3.6	4.6	6.7	5.4
$10H$	5.2	6.0	5.6	2.5	3.8	6.0	4.1
av_1	11.5	11.7	11.8	9.9	10.3	10.0	10.3
av_2	6.9	7.6	7.5	4.5	5.3	7.1	5.5
av	9.2	9.6	9.6	7.2	7.8	8.5	7.9
u_2	$1ns$	$1ns + 1ws(H)$	$1ns + 1ws(2H)$	$2ns$	$2ns + 2ws(2H)$	$2ns + 1ws(2H), d$	$2ns + 1ws(2H), b$
$3H$	13.1	12.7	12.8	12.6	12.5	11.7	12.3
$4H$	10.2	10.4	10.8	9.4	9.5	9.4	9.8
$5H$	9.8	9.7	10.0	8.8	9.5	9.1	8.4
$6H$	8.3	7.9	8.8	7.1	6.8	8.7	7.4
$7H$	5.2	6.5	6.2	4.5	3.9	7.7	4.9
$8H$	4.8	6.1	6.0	2.8	3.6	6.9	4.6
$9H$	2.9	4.9	4.9	1.0	2.2	5.8	2.8
$10H$	1.6	3.9	4.0	0.2	1.9	4.4	2.2
av_1	10.3	10.2	10.6	9.5	9.6	9.7	9.5
av_2	3.6	5.4	5.3	2.1	2.9	6.2	3.6
av	7.0	7.8	7.9	5.8	6.2	8.0	6.6

time wind speeds higher than 5 m/s (averaged over a period of one minute) occur. Even wind speeds higher than 10 m/s can be measured 5% of the time close to the surface.

The effect of wind on the barrier performance is significant (see Table I and Figure 5). Close to the barrier (from $3H$ till $6H$), only small differences in IL arise. The wind tunnel experiments of DeJong and Stusnick confirm these results [3]. At greater distances, the wind effect becomes important. Quantitative agreement with other experiments is also found [1]. With increasing wind speed, the performance of the noise barriers becomes worse. A decrease of more than 10 dB in barrier performance for a normal incident wind of 11 m/s is observed.

For a double screen, almost the same trends are noticed. The overall performance for this case in absence of wind is worse, due to reflection on the screen located upwind of the noise source. For the highest wind speed in the experiment, at a distance of 10 times the barrier height behind the downwind screen, the use of a noise screen becomes almost useless. It has to be mentioned however that part of the decrease in insertion loss has its origin in the reference situation, i.e. propagation in wind without screens. It is observed that sound levels decrease considerably with increasing wind speed (see Figure 6). This phenomenon is

Table II. Net IL (in dB) by the windscreens at the test distances (expressed in screen heights), together with the averages over the first part ($av_1 = 3H$–$6H$) and second part ($av_2 = 7H$–$10H$) of the test section, and a global average (av= $3H$–$10H$). A windless situation ($= u_0$) and two wind speeds, measured above the boundary layer, are used: $u_1 = 6.4$ m/s and $u_2 = 11$ m/s.

	$1ns + 1ws(H)$			$1ns + 1ws(2H)$			$2ns + 2ws(2H)$			$2ns + 1ws(2H), d$			$2ns + 1ws(2H), b$		
	u_0	u_1	u_2	u_0	u_1	u_2	u_0	u_1	u_2	u_0	u_1	u_2	u_0	u_1	u_2
$3H$	0.2	-0.2	-0.4	-0.1	0.5	-0.3	-0.2	0.5	0.0	-0.3	-0.7	-0.9	-0.4	0.0	-0.3
$4H$	0.0	-0.3	0.2	0.8	-0.2	0.6	0.9	0.5	0.1	0.9	1.2	0.0	0.3	0.4	0.4
$5H$	-0.5	0.9	-0.1	-0.4	0.5	0.2	-1.3	0.4	0.7	-0.2	-0.4	0.3	-0.6	0.6	-0.4
$6H$	0.2	0.4	-0.4	0.0	0.4	0.5	-0.2	-0.1	-0.3	0.1	0.0	1.6	0.0	0.2	0.3
$7H$	0.4	0.8	1.2	-0.4	0.9	1.0	-0.8	-0.2	-0.6	-0.1	1.0	3.1	-0.4	-0.6	0.4
$8H$	0.1	0.3	1.3	0.4	0.0	1.1	0.6	1.0	0.8	1.0	2.5	4.2	0.4	1.0	1.8
$9H$	0.6	1.0	2.0	0.2	1.1	2.0	0.7	1.0	1.2	-0.4	3.1	4.8	-0.1	1.8	1.9
$10H$	0.2	0.8	2.3	-0.9	0.4	2.4	-0.1	1.2	1.7	0.6	3.5	4.2	0.1	1.6	2.0
av_1	0.0	0.2	-0.2	0.1	0.3	0.3	-0.2	0.3	0.1	0.1	0.0	0.3	-0.2	0.4	-0.1
av_2	0.3	0.7	1.7	-0.2	0.6	1.6	0.1	0.8	0.8	0.3	2.5	4.1	0.0	0.9	1.5
av	0.2	0.4	0.8	0.0	0.4	0.9	0.0	0.5	0.4	0.2	1.3	2.2	-0.1	0.6	0.8

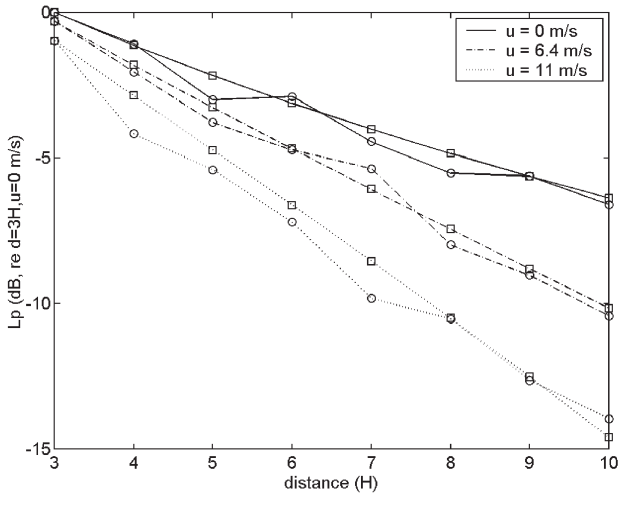

Figure 6. Sound pressure levels in the wind tunnel, in absence of both noise barriers and windscreens, with increasing distances (expressed in screen heights, downwind from the place where the noise barrier will be placed) and for different wind speeds (measured above the boundary layer). The sound pressure levels are given relative to the first measurepoint (at a distance of $3H$) in absence of wind. The measured sound pressure levels are indicated by the circles, the simulated sound pressure levels by the squares.

a consequence of the use of a source at ground level. The analogy to a free propagation overanalyse.

To model sound propagation over a finite impedance ground in a refractive atmosphere, the analogy to free propagation over a curved ground surface can be used in a first approximation [17]. In this respect, downward refraction caused by the strong gradients in wind speed near the surface can be modeled by a source situated on a virtual hill. For higher wind speeds, the curvature of the surface increases. Therefore destructive interference between direct and reflected waves can increase within the frequency range of interest, explaining the larger reduction of sound pressure levels. The measured sound pressure levels, relative to the first measurepoint in absence of wind, are shown together with the slopes, simulated using this model, in Figure 6. For a wind speed of 6.4 m/s measured above the boundary layer, a curvature of the ground surface with radius at full scale of 0.49 km is used to fit the measured data, for 11 m/s a smaller radius of 0.37 km is obtained. This very simple model explains, at least qualitatively, the observed behaviour.

When investigating the net effect of the windscreens, the insertion losses of the configurations with a windscreen are compared to the same noise barrier configurations without windscreens. These results are given in Table II. At small distances, the net effect of the windscreens is small, and sometimes slightly negative. This effect can be attributed to scattering on the windscreen. For the cases with wind, also scattering by turbulent flow near the screens may be changed by the windscreen and could result in negative net effects. At larger distances, the net effect of the windscreens is always positive.

When comparing one noise screen with a low ($1H$, $1ns + 1ws(H)$) and a high ($2H$, $1ns + 1ws(2H)$) vegetation screen, there's not much difference between them. It seems that it's only the zone just above the barrier that needs to be shielded to improve the insertion loss.

For the case with 2 noise barriers, and a windscreen of 2 times the barrier height placed behind the barrier closest to the receiver ($2ns + 1ws(2H), d$), an average improvement of 4 dB is obtained at larger distances. This configuration seems to be the most efficient among the tested ones. It is also observed that a good modification of the wind speed profile is not straightforward. For the configuration, consisting of 2 noise barriers with two high windscreens ($2ns + 2ws(2H)$), the performance is worse than for the case where only a single windscreen is used ($2ns + 1ws(2H), d$). A more detailed analysis of this situation can be found in section 3.2.

The used screens are in the path of the sound passing just over the barrier. In absence of wind, absorption by trees and porous windscreens is expected to be very small. In wind, theoretical calculations predict a larger absorption by perforated screens. It is investigated to what extent this excess absorption of sound by the windscreens in wind is important in the total effect of the windscreens. The use of a perforated screen provides absorption of acoustic energy by vorticity production. This effect is more pronounced in flow, since this generated vorticity is flown away. In this way, a certain amount of energy of the sound wave is permanently lost [18]. This effect can be quantified as proposed in reference [18]. Just before the windscreens, the average horizontal wind velocity component is not larger than 5 m/s in all of the situations considered here. It is calculated that for an (average) incident angle of 45 degrees, the absorption of acoustic energy by the perforated screen is not larger than 4%. This means that for the net effect of the windscreens, only 0.17 dB can be assigned to this effect. Therefore it is concluded that the positive effect of the windscreens is caused mainly by an improved wind profile.

3.2. Detailed analysis of a double noise barrier with a single and a double windscreen

To analyse the difference in improvement of the double barrier performance in wind when one or two windscreens are used, the flow field is modeled with the CFD software package STAR-CD. Calibration has been done using the experimental velocities for the case with 2 noise barriers without windscreens ($2ns$), for a free-stream flow velocity of 11 m/s. This calibration is based only on the positive horizontal components of the flow velocity since the vertical and negative horizontal component can not be measured with the available anemometers. This procedure will still be quite accurate, since the vertical components are only important close to the screens. Recirculating flows on the other hand are only present close to the surface.

Every measurement lasted 1 minute, with a sample frequency of 1 Hz. This is necessary since the flow in the wind tunnel is turbulent. For further comparison, the time-averaged values are used. The standard deviation on the velocity measurements has an average value of about 0.3 m/s. The best correspondence between wind velocity calculations and experimental data is obtained by using a steady state, k-ε turbulence flow model. At most places, the differences between simulated and measured values are below 1 m/s. Taking into account the time dependency of the flow, this is a good approximation.

As an illustration, the measured wind profiles at 10 locations and 5 heights are given in Figure 7 for the configuration with two noise barriers and two high windscreens ($2ns + 2ws(2H)$). The 95% confidence intervals are indicated in this figure for every measurement, assuming a normal distribution of the velocities during the measurements.

At first sight, one could expect that the more wind speed is reduced (by placing additional windscreens), the higher the improvement in noise barrier performance under wind conditions. The experiments reveal however that a double noise barrier configuration with one downwind windscreen is significantly better than the same situation with two windscreens. A comparison of the simulated (horizontal) wind velocity field at some locations near the noise barriers in the wind tunnel in both situations is given in Figure 8.

Acoustic ray paths can be traced in these flow profiles and it is clear that they will refract both upward and downward. The important difference between wind gradients in the source region for both configurations makes it plausible that refraction and therefore insertion loss differs considerably. However, at this moment, quantitative agreement with measured insertion loss could not be found.

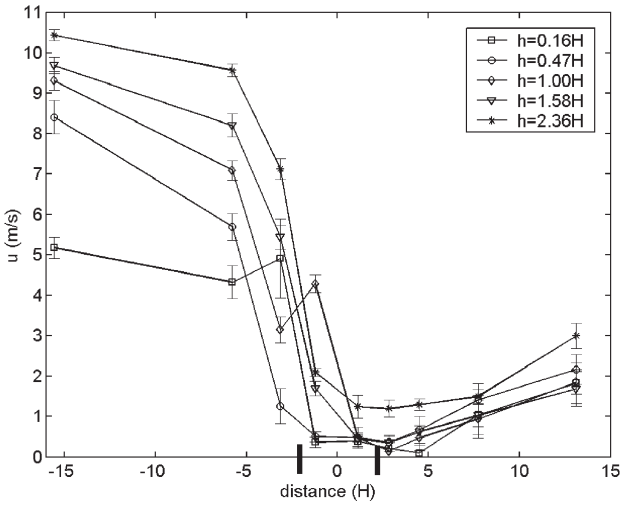

Figure 7. Measured wind speed profiles at different locations. Distances (relative to the position of the source) and heights are expressed in screen heights. The wind velocity above the boundary layer is 11 m/s. Configuration ($2ns + 2ws(2H)$) is used. The location of the noise barriers is indicated with the black lines on the distance scale.

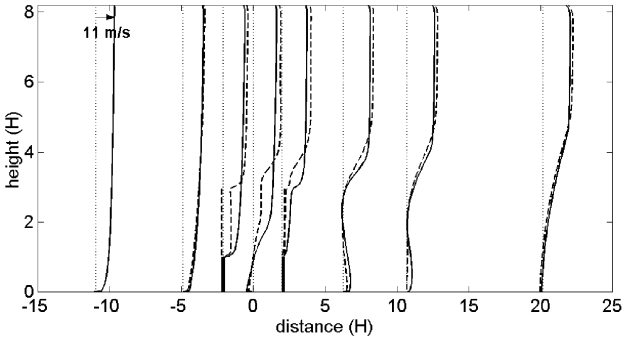

Figure 8. Wind speeds profiles along the wind tunnel at selected locations. The incident wind velocity above the boundary layer is 11 m/s. Distances (relative to the position of the source) and heights are expressed in screen heights. The velocity profiles for configuration $2ns + 2ws(2H)$ are represented by the dashed lines, for configuration $2ns + 1ws(2H)$, d the full lines are used. For each profile, the line of zero wind speed is indicated with the dotted lines.

Moreover, additional factors may contribute to the effect. The stronger quasi-static pressure drop and larger velocity gradients at the downwind screen in the situation were only one windscreen is present could result in a partial reflection at this screen. This example illustrates that designing the wind profiles for optimal noise barrier performance is possible, but also that it is not a trivial task. Detailed numerical analysis is required.

4. Conclusions

In this paper, a solution to weaken downward refraction by wind gradients behind a noise barrier is proposed. Different configurations of single and double noise barriers, with vegetative screens are investigated in a wind tunnel experiment. The net effect of the vegetative screens is positive (an improvement up to 4 dB), but its magnitude depends on the configuration used. With increasing distances behind the barrier and wind speed, this improvement becomes more prominent. A good modification of wind profiles to improve barrier performance is however not always straightforward. For double noise barriers for example, the use of one windscreen (behind the downwind noise barrier) instead of two windscreens results in a better modification of the wind profile. Although the improvement of noise barrier performance in wind by placing additional windscreens is not more than a few dB, the additional cost for planting trees and bushes that can act as a windscreen, is not high. Therefore, these first results can lead to interesting practical applications. Problems however may arise when using real trees, especially to obtain an optimal porosity of the canopy throughout the year. Further research will have to include a complete numerical analysis of sound propagation near sound barriers equiped with windscreens.

Acknowledgements

The authors are grateful to the anonymous reviewers, for their many helpful suggestions when reviewing this paper. Also W. Dierickx needs to be thanked, for kindly providing the paper he wrote on the windscreens used in the experiment and useful comments on this topic.

References

[1] E. M. Salomons: Reduction of the performance of a noise screen due to screen-induced wind-speed gradients. Numerical computations and wind tunnel experiments. J. Acoust. Soc. Am. **105** (1999) 2287–2293.

[2] G. A. Daigle, J. E. Piercy, T. F. W. Embleton: Effects of atmospheric turbulence on the interference of sound waves near a hard boundary. J. Acoust. Soc. Am. **64** (1978) 622–630.

[3] R. DeJong, E. Stusnick: Scale model studies of the effect of wind on acoustic barrier performance. Noise control engineering **6** (1976) 101–109.

[4] K. B. Rasmussen: Sound propagation over screened ground under upwind conditions. J. Acoust. Soc. Am. **100** (1996) 3581–3586.

[5] K. B. Rasmussen, M. G. Arranz: The insertion loss of screens under the influence of wind. J. Acoust. Soc. Am. **104** (1998) 2692–2698.

[6] N. Barriere, Y. Gabillet: Sound propagation over a barrier with realistic wind gradients. Comparison of wind tunnel experiments with GFPE computations. Acustica–Acta acustica **85** (1999) 325–334.

[7] E. M. Salomons: Reduction of the performance of a noise screen due to screen-induced wind-speed gradients. Numerical computations and wind tunnel experiments. J. Acoust. Soc. Am. **105** (1999) 2287–2293.

[8] E. M. Salomons, K. B. Rasmussen: Numerical computations of sound propagation over a noise screen based on an analytic approximation of the wind speed field. Appl. Acoustics **60** (2000) 327–341.

[9] G. A. Daigle: Diffraction of sound by a noise barrier in the presence of atmospheric turbulence. J. Acoust. Soc. Am. **71** (1982) 847–854.

[10] T. Meloni, F. Fischer: Factors moderating the effect of noise barriers. Proceedings of NOISE-CON, Newport Beach, USA, 2000.

[11] D. Gabriels, W. Cornelis, I. Pollet, T. Van Coillie, M. Ouessar: The I.C.E. wind tunnel for wind and water erosion studies. Soil Technology **10** (1997) 1–8.

[12] J. E. Piercy, T. Embleton, L. Sutherland: Review of noise propagation in the atmosphere. J. Acoust. Soc. Am. **61** (1977) 1403–1418.

[13] M. Delaney, E. Bazley: Acoustical properties of fibrous absorbent materials. Applied Acoustics **3** (1970) 105–116.

[14] W. M. Cornelis, D. Gabriels, T. Lauwaerts: Simulation of windbreaks for wind-erosion control in a wind tunnel. Proceedings of Wind Erosion, Manhattan, USA, 1999.

[15] W. Dierickx: Flow reduction of synthetic screens obtained with both a water and airflow apparatus. J. Agric. Eng. Res. **71** (1998) 67–73.

[16] STAR-CD (version 3.100A). Computational dynamics LTD, London, 2000.

[17] T. F. W. Embleton: Analogies between nonflat ground and nonuniform meteorological profiles in outdoor sound propagation. J. Acoust. Soc. Am. **78** (1985) S86.

[18] M. S. Howe: Acoustics of fluid-structure interactions (chapter 5.3 “interactions with perforated screens”). Cambridge University press, 1998.